Decomposition of the wave field into optimized Gaussian packets

Karel Žáček

Department of Geophysics, Charles University, Ke Karlovu 3, 121 16 Praha 2, Czech Republic, E-mail: zacek@karel.troja.mff.cuni.cz

Summary

The decomposition of the wave field into optimized Gaussian packets is of key importance in the Gaussian packet migration. We present the theoretical basics and the first numerical examples of our method.

Key words

Gaussian packets, coherent–state transform, migration.

1 Introduction

Our long–term project is to explore the properties of a depth migration method based on Gaussian packets. Gaussian packets (GPs) are waves whose envelopes at any given time are *nearly* Gaussian in space. They represent high–frequency asymptotic solutions of the elastodynamic equation, which are concentrated close to the central point of the packet (e.g, Babich & Ulin, 1981, Ralston, 1983, Klimeš, 1989a).

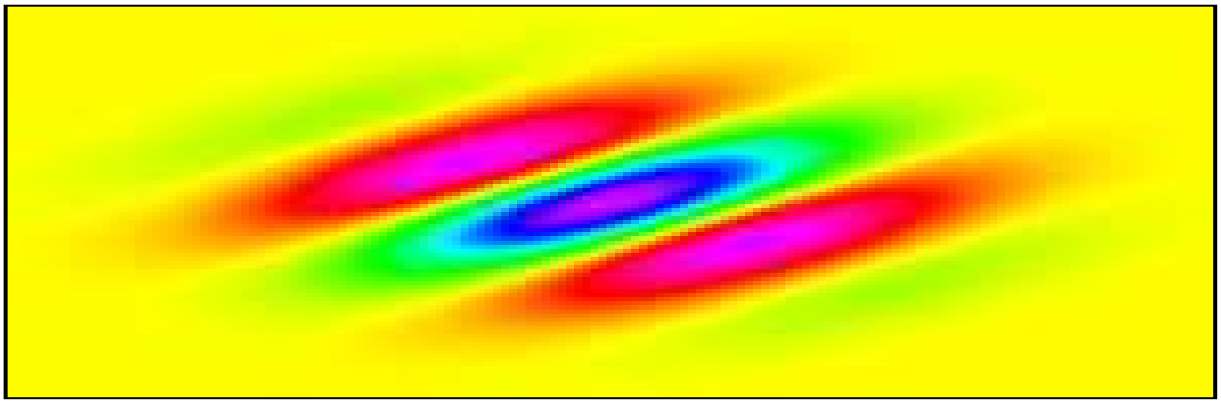

Figure 1. A Gaussian packet.

The advantages over the methods based on Gaussian beams should consist in increased accuracy, computational efficiency and a direct relation between the regions in the common shot gather and corresponding regions in the migrated section.

As well as Gaussian beams, GPs become inaccurate solutions of the elastodynamic equation if they spread excessively as they propagate. This spreading depends on the complexity of the velocity model and on the initial shape of GPs. Thus, we should use a sufficiently smooth velocity model and *optimize* the initial shape of the packets.

The GP migration algorithm consists of five basic steps:
a) Preparation of a suitable smooth velocity model (e.g., Žáček, 2002).
b) Optimization of the shape of GPs (Klimeš, 1989b, Žáček, 2001).

In: Seismic Waves in Complex 3–D Structures, Report 13 (Department of Geophysics, Charles University, Prague, 2003), pp.35–43

c) Decomposition of the wave field (common shot gather) into optimized GPs.
d) Back–propagation of the wave field using GPs.
e) Application of the imaging function.

Currently, we are dealing with the decomposition of the wave field into *optimized* GPs. The word *optimized* means that the shape of GPs depends not only on the frequency, but also on the coordinate of the intersection of the central ray of a GP with the profile, on its arrival time, and on the component of the slowness vector along the profile.

2 Basic theory

We would like to approximate the "time section" (common shot gather) $f(x,t)$ in the form of

$$\widetilde{f}(x',t') = \int \mathrm{d}t_\mathrm{R} \int \mathrm{d}\omega \, \exp\left[-\mathrm{i}\omega(t'-t_\mathrm{R})\right] \int \mathrm{d}x_\mathrm{R} \int \mathrm{d}p \, \exp\left[\mathrm{i}\omega p(x'-x_\mathrm{R})\right]$$

$$\times \; W(x'-x_\mathrm{R}, t'-t_\mathrm{R}, x_\mathrm{R}, p, t_\mathrm{R}, \omega) \; F(x_\mathrm{R}, p, t_\mathrm{R}, \omega) \quad , \tag{1}$$

where x_R is the coordinate and t_R is the time of the intersection of the central ray of a GP with the profile, p is the component of the slowness vector along the profile, ω is the positive circular frequency of a GP, W determines the shape of the envelope of a GP, and the complex–valued function $F(x_\mathrm{R}, p, t_\mathrm{R}, \omega)$ specifies the amplitude of a GP.

Let us express the amplitude of a GP in the form of an integral transform similar to the forward 2–D *coherent–state transform*,

$$F(x_\mathrm{R}, p, t_\mathrm{R}, \omega) = \frac{\omega}{(2\pi)^2} \int \mathrm{d}x \, \exp\left[-\mathrm{i}\omega p(x-x_\mathrm{R})\right] \int \mathrm{d}t \, \exp\left[\mathrm{i}\omega(t-t_\mathrm{R})\right]$$

$$\times \; w(x_\mathrm{R}-x, t_\mathrm{R}-t, x_\mathrm{R}, p, t_\mathrm{R}, \omega) \; f(x,t) \quad . \tag{2}$$

The envelope of the trace of a GP along the profile may be expressed as

$$W(x'-x_\mathrm{R}, t'-t_\mathrm{R}, x_\mathrm{R}, p, t_\mathrm{R}, \omega) = \exp\left[\mathrm{i}\omega\frac{1}{2}(\mathbf{y}'-\mathbf{y}_\mathrm{R})^\mathrm{T}\mathbf{K}(\mathbf{y}'-\mathbf{y}_\mathrm{R})\right] \quad , \tag{3}$$

where

$$\mathbf{y}' = \begin{pmatrix} x' \\ t' \end{pmatrix} \quad , \tag{4}$$

$$\mathbf{y}_\mathrm{R} = \begin{pmatrix} x_\mathrm{R} \\ t_\mathrm{R} \end{pmatrix} \tag{5}$$

and

$$\mathbf{K} = N \begin{pmatrix} 1 & 0 \\ 0 & 0 \end{pmatrix} + N_{44} \begin{pmatrix} p^2 & -p \\ -p & 1 \end{pmatrix} \quad . \tag{6}$$

Let us write the analyzing functions in an analogous form,

$$w(x'-x_\mathrm{R}, t'-t_\mathrm{R}, x_\mathrm{R}, p, t_\mathrm{R}, \omega) = \widetilde{a} \, \exp\left[\mathrm{i}\omega\frac{1}{2}(\mathbf{y}-\mathbf{y}_\mathrm{R})^\mathrm{T}\widetilde{\mathbf{K}}(\mathbf{y}-\mathbf{y}_\mathrm{R})\right] \quad , \tag{7}$$

where

$$\widetilde{a} = \frac{\omega}{2\pi}\sqrt{-\mathrm{i}(N+\widetilde{N})}\sqrt{-\mathrm{i}N_{44}\widetilde{N}_{44}\left(\frac{\omega}{K_0}+\frac{\omega}{\widetilde{K}_0}\right)} \quad , \tag{8}$$

the square roots should be taken with positive real parts,

$$\mathbf{y} = \begin{pmatrix} x \\ t \end{pmatrix} \quad , \tag{9}$$

and

$$\widetilde{\mathbf{K}} = \widetilde{N}\begin{pmatrix} 1 & 0 \\ 0 & 0 \end{pmatrix} + \widetilde{N}_{44}\begin{pmatrix} \widetilde{p}^2 & -\widetilde{p} \\ -\widetilde{p} & 1 \end{pmatrix} \quad . \tag{10}$$

Parameters determining the forward and inverse transformation must satisfy

$$\frac{1}{N}+\frac{1}{\widetilde{N}} = \frac{2}{N_0} \quad , \tag{11}$$

$$\frac{p}{N}+\frac{\widetilde{p}}{\widetilde{N}} = 0 \tag{12}$$

and

$$\frac{p^2}{N}+\frac{1}{N_{44}}+\frac{\widetilde{p}^2}{\widetilde{N}}+\frac{1}{\widetilde{N}_{44}} = \frac{\omega}{K_0}+\frac{\omega}{\widetilde{K}_0} \quad , \tag{13}$$

where N_0, K_0 and $\widetilde{K}_0$ are free constants to be set by the user. They may be generally complex–valued, but we choose K_0 and $\widetilde{K}_0$ as pure imaginary only.

A complex–valued parameter N determines the initial shape of GPs. To avoid an excessive spreading of GPs, we should use *optimized* GPs,

$$N = N(x_\mathrm{R}, t_\mathrm{R}, p) \quad . \tag{14}$$

Optimized parameters may be obtained as described by Žáček (2001). In this place, we must point out that the transformation is exact,

$$\widetilde{f}(x,t) = f(x,t) \quad , \tag{15}$$

only for N independent on x_R and t_R. Thus, using *optimized* GPs is strictly mathematically speaking incorrect. However, for reasonably smooth distribution of N with respect to x_R and t_R, we could get satisfactory results.

Using equation (11) and (12), we may write

$$\widetilde{N} = \frac{NN_0}{2N-N_0} \tag{16}$$

and

$$\widetilde{p} = -\frac{\widetilde{N}}{N}p \quad . \tag{17}$$

Please note that parameter p is real–valued, but $\widetilde{p}$ is generally complex–valued.

Equation (13) may be rearranged in several ways to determine parameters N_{44} and $\widetilde{N}_{44}$. For instance, we can get two symmetrical expresions,

$$\widetilde{N}_{44} = \frac{\widetilde{N}\widetilde{K}_0}{\omega\widetilde{N}-\widetilde{p}^2\widetilde{K}_0} \quad , \tag{18}$$

$$N_{44} = \frac{N K_0}{\omega N - p^2 K_0} \quad . \tag{19}$$

Then, pure imaginary constants $\widetilde{K}_0$ and K_0 must obey

$$\mathrm{Im}(\widetilde{K}_0) < \mathrm{Im}\left(\frac{\omega_{\mathrm{MIN}}\widetilde{N}_{\mathrm{MIN}}}{\widetilde{p}^2_{\mathrm{MAX}}}\right) \quad , \tag{20}$$

$$\mathrm{Im}(K_0) < \mathrm{Im}\left(\frac{\omega_{\mathrm{MIN}} N_{\mathrm{MIN}}}{p^2_{\mathrm{MAX}}}\right) \quad . \tag{21}$$

Another approach would allow the use of the fast Fourier transform (FFT) in the decomposition of the wave field,

$$\widetilde{N}_{44} = \frac{\widetilde{K}_0}{\omega} \quad , \tag{22}$$

$$N_{44} = \left(\frac{\omega}{K_0} - \frac{p^2}{N} - \frac{\widetilde{p}^2}{\widetilde{N}}\right)^{-1} \quad , \tag{23}$$

$$\mathrm{Im}(K_0) < \mathrm{Im}\left(\frac{\omega_{\mathrm{MIN}}\,(2N_{\mathrm{MIN}} - N_0)}{p^2_{\mathrm{MAX}}}\right) \quad . \tag{24}$$

Maximum steps in x_{R}, t_{R}, p and ω for replacement of integral (1) by its discretized counterpart are

$$\Delta x_{\mathrm{R}} = \kappa\sqrt{-\frac{2}{\omega}\left[\mathrm{Im}\left((\mathbf{K}+\widetilde{\mathbf{K}})^{-1}\right)\right]_{11}} \quad , \tag{25}$$

$$\Delta t_{\mathrm{R}} = \kappa\sqrt{-\frac{2}{\omega}\left[\mathrm{Im}\left((\mathbf{K}+\widetilde{\mathbf{K}})^{-1}\right)\right]_{22}} \quad , \tag{26}$$

$$\Delta p = \kappa\sqrt{\frac{2}{\omega}\left[\mathrm{Im}\left((\mathbf{K}^{-1}+\widetilde{\mathbf{K}}^{-1})^{-1}\right)\right]_{11}} \tag{27}$$

and

$$\Delta \omega = \kappa\sqrt{2\omega\left[\mathrm{Im}\left((\mathbf{K}^{-1}+\widetilde{\mathbf{K}}^{-1})^{-1}\right)\right]_{22}} \quad . \tag{28}$$

Reasonable values of κ range from $\kappa^2 = 1$ through $\kappa^2 = \frac{\pi}{2}$ to $\kappa^2 = \pi$. We expect $\kappa^2 = \pi$ to be a practical compromise between the price and accuracy in the migration.

Equations (27) and (28) yield

$$\Delta p = \kappa\sqrt{\frac{\mathrm{Im}(N_0)}{\omega_{\mathrm{MAX}}}} \tag{29}$$

and

$$\Delta \omega = \kappa\sqrt{2\ \mathrm{Im}\left(\frac{K_0\widetilde{K}_0}{K_0+\widetilde{K}_0}\right)} \quad . \tag{30}$$

We shall not forget that maximum steps in p and ω for the Fourier transform are

$$(\Delta p)_{\mathrm{FT}} = \frac{2\pi}{N_{\mathrm{x}}\ \Delta x\ \omega} \tag{31}$$

and

$$(\Delta \omega)_{\mathrm{FT}} = \frac{2\pi}{N_{\mathrm{t}}\ \Delta t} \quad , \tag{32}$$

where N_x and N_t are the numbers of samples in space and time, respectively. To avoid aliasing, we must keep the steps below criterions (31) and (32).

Analytical expressions for Δx_R and Δt_R are generally complicated and we do not present them. However, we can introduce a new parametrization of our task and estimate them. According to equations (16), (20) and (21), we may write

$$N_0 = 2\nu N_\mathrm{MIN} \quad , \tag{33}$$

$$K_0 = \mathrm{i}\ \xi \frac{\omega_\mathrm{MIN}\mathrm{Im}(N_\mathrm{MIN})}{p^2_\mathrm{MAX}} \tag{34}$$

and

$$\widetilde{K}_0 = \mathrm{i}\ \xi \frac{1-\nu}{\nu} \frac{\omega_\mathrm{MIN}\mathrm{Im}(N_\mathrm{MIN})}{p^2_\mathrm{MAX}} \quad , \tag{35}$$

where

$$\nu \in (0,1) \quad , \tag{36}$$

$$\xi \in (0,1) \quad . \tag{37}$$

Now, we can estimate the maximum steps in x_R and t_R as

$$\Delta x_\mathrm{R} \approx \kappa \sqrt{-\frac{2(1-\nu)}{\omega_\mathrm{MAX}} \mathrm{Im}\left[\frac{\left(1 - \frac{\mathrm{i}\ \mathrm{Im}(N_\mathrm{MIN})}{N_\mathrm{MAX}} \frac{\omega_\mathrm{MIN}}{\omega_\mathrm{MAX}} \xi\right)}{N_\mathrm{MAX}}\right]} \tag{38}$$

and

$$\Delta t_\mathrm{R} \approx \kappa \sqrt{-\frac{2\nu p^2_\mathrm{MAX}}{\omega_\mathrm{MIN}} \mathrm{Im}\left[\frac{\left(1 - \frac{\mathrm{i}\ \mathrm{Im}(N_\mathrm{MIN})}{N_\mathrm{MIN}} \xi\right)}{\mathrm{i}\ \xi \mathrm{Im}(N_\mathrm{MIN})}\right]} \quad , \tag{39}$$

which yields

$$\Delta t_\mathrm{R} \approx \kappa \sqrt{-2\nu \mathrm{Im}\left[\frac{\left(1 - \frac{\mathrm{i}\ \mathrm{Im}(N_\mathrm{MIN})}{N_\mathrm{MIN}} \xi\right)}{K_0}\right]} \quad . \tag{40}$$

Please keep in mind that these estimates are valid only for N_{44} and $\widetilde{N}_{44}$ determined by equations (18) and (19). Nevertheless, we can easily perform analogous calculations for equations (22) and (23) or for any other choice of parameters N_{44} and $\widetilde{N}_{44}$.

3 Numerical examples

We tested our method on a common shot gather belonging to the Marmousi data set (Versteeg & Grau, 1991), see Figure 2. We decomposed the gather $f(x,t)$ using equation (2) into GPs and obtained the complex–valued amplitudes $F(x_\mathrm{R},p,t_\mathrm{R},\omega)$. Then, we composed the approximated common shot gathers $\widetilde{f}(x,t)$ according to equation (1), see Figure 3. The differences between the original gather and the approximated gathers are displayed in Figure 4. We used $\kappa^2 = \pi$ in all calculations.

The first example is the decomposition into *uniform* GPs. The word *uniform* means that

$$N = \widetilde{N} = N_0 \quad . \tag{41}$$

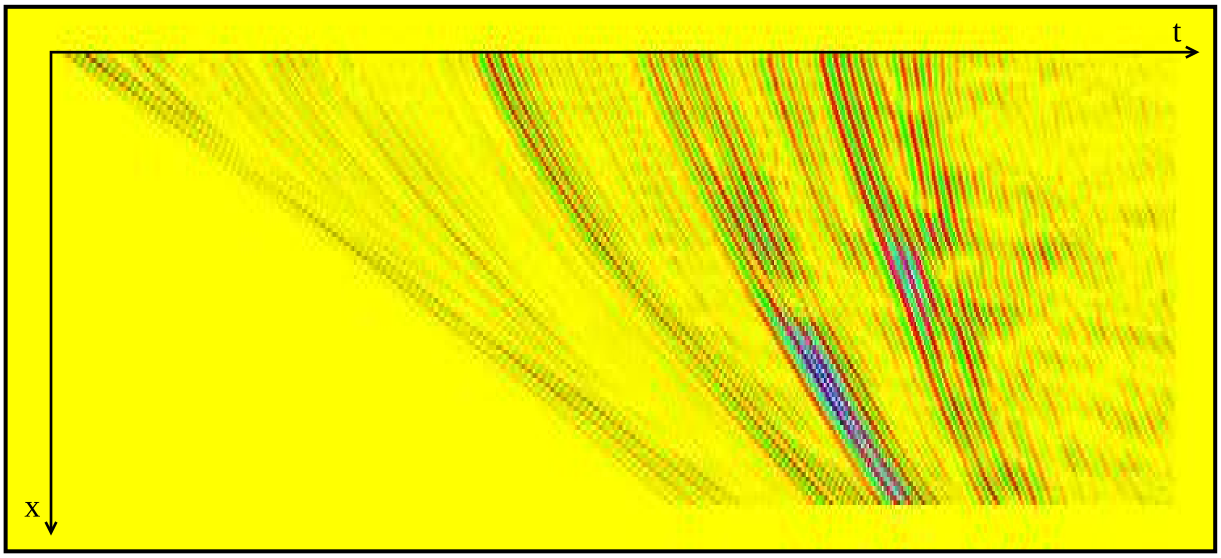

Figure 2. Common shot gather $f(x,t)$.

We choose $\mathrm{Re}(N_0) = -0.25 \times 10^{-6}$ sm^{-2} and $\mathrm{Im}(N_0) = 0.25 \times 10^{-6}$ sm^{-2}. See Figure 3a for the corresponding approximated common shot gather. Figure 4a indicates that the transformation is almost exact.

The next example demostrates the decomposition of the wave field into *optimized* GPs. In this case, $\mathrm{Re}(N) = -0.25 \times 10^{-6}$ sm^{-2}, $\mathrm{Im}(N)$ ranging from 0.125×10^{-6} sm^{-2} to 0.5×10^{-6} sm^{-2}, $\nu = 0.5$ and $\xi = 0.1$. The approximated gather is shown in Figure 3b. According to Figure 4b, the differences between the original and the approximated wave fields can be spotted not only at the edges of the gather. This is caused by the dependency of parameter N on x_{R} and t_{R}.

The last example is the decomposition for $\mathrm{Re}(N) = -0.25 \times 10^{-6}$ sm^{-2}, $\mathrm{Im}(N)$ ranging from 0.75×10^{-7} sm^{-2} to 0.1×10^{-5} sm^{-2}, $\nu = 0.5$ and $\xi = 0.3$. The approximated gather is displayed in Figure 3b. Although we can note several differences between the original and the approximated gathers in Figure 4c, the result is not completely wrong. Furthermore, we could improve it (in dependency upon the computer power we dispose) by using $\kappa^2 = \frac{\pi}{2}$ or even $\kappa^2 = 1$.

The only serious problem of our method we encounter is the computational cost. Unfortunately, we cannot use 2–D FFT. The mathematical formulation of our task allows only a series of 1–D FFTs in the decomposition, but not in the composition. However, we are permanently trying to refine the algorithm and speed up the computations.

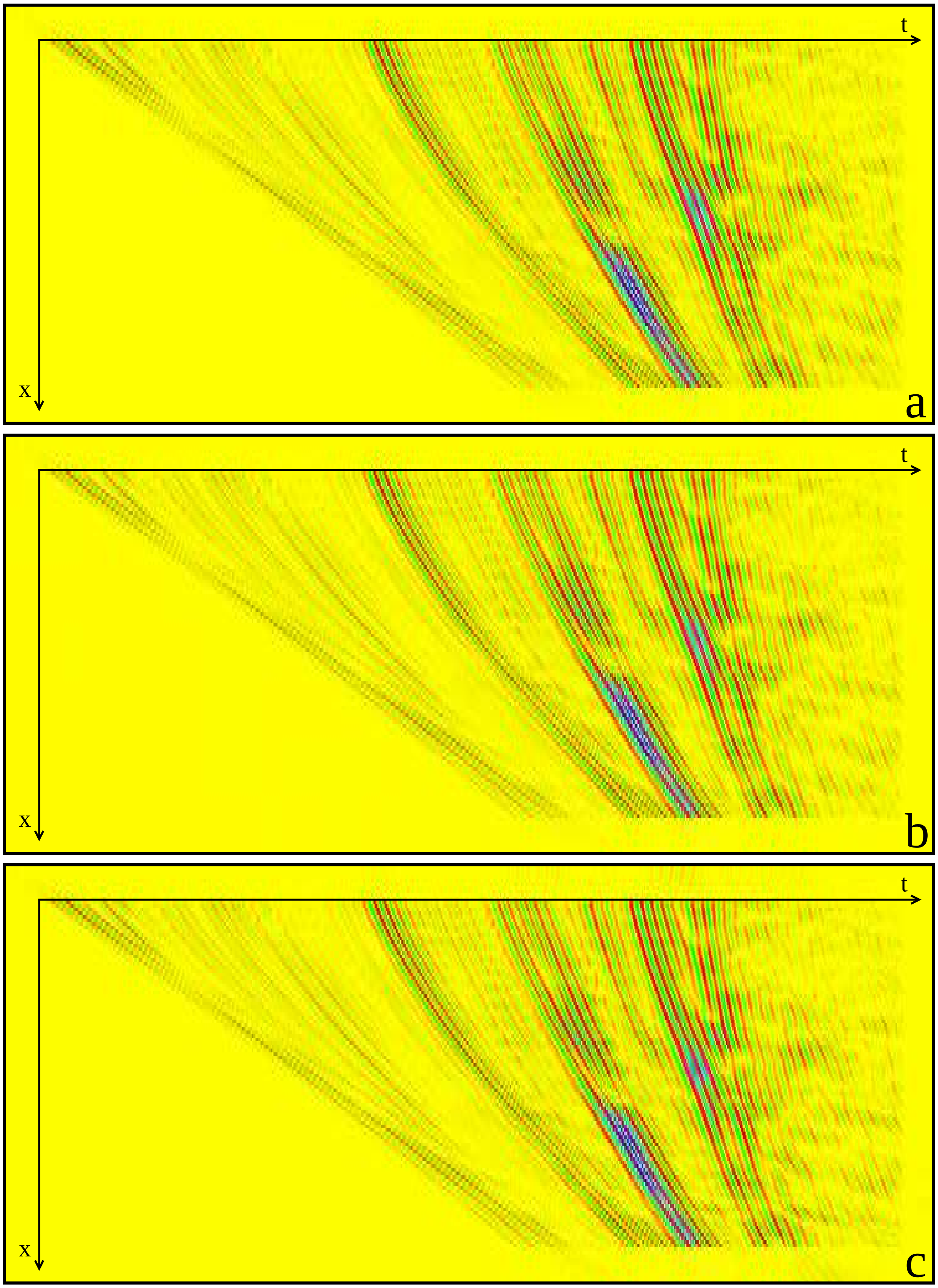

Figure 3. Approximated common shot gathers $\widetilde{f}(x,t)$ for (a) *uniform* GPs, (b) *optimized* GPs ($\mathrm{Re}(N) = -0.25 \times 10^{-6}$ sm^{-2}, $\mathrm{Im}(N)$ ranging from 0.125×10^{-6} sm^{-2} to 0.5×10^{-6} sm^{-2}), and (c) *optimized* GPs ($\mathrm{Re}(N) = -0.25 \times 10^{-6}$ sm^{-2}, $\mathrm{Im}(N)$ ranging from 0.75×10^{-7} sm^{-2} to 0.1×10^{-5} sm^{-2}).

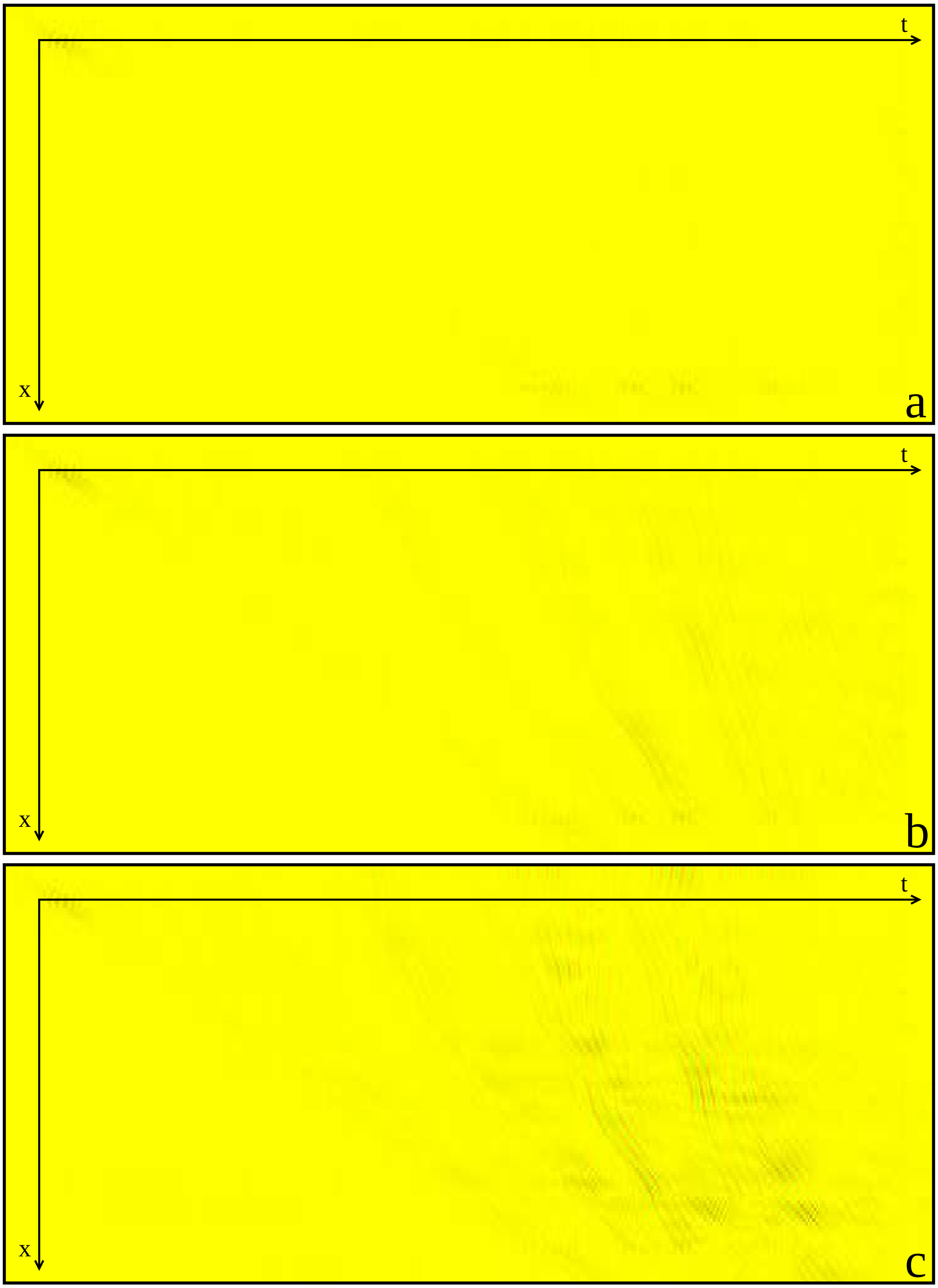

Figure 4. Differences between the original common shot gather $f(x,t)$ and the approximated common shot gathers for (a) *uniform* GPs, (b) *optimized* GPs ($\mathrm{Re}(N) = -0.25 \times 10^{-6}$ sm^{-2}, $\mathrm{Im}(N)$ ranging from 0.125×10^{-6} sm^{-2} to 0.5×10^{-6} sm^{-2}), and (c) *optimized* GPs ($\mathrm{Re}(N) = -0.25 \times 10^{-6}$ sm^{-2}, $\mathrm{Im}(N)$ ranging from 0.75×10^{-7} sm^{-2} to 0.1×10^{-5} sm^{-2}).

4 Conclusions

The presented procedure of the decomposition of the wave field into Gaussian packets is fully functional. It might be suitable not only for Gaussian packet migration, but also for many different applications of the Gaussian packet method.

The main disadvantage of our approach seems to be the computational cost of the decomposition. Nevertheless, once we obtain the amplitudes of Gaussian packets, we can calculate many migrated sections for various (reasonably similar) velocity models.

The next step in our research will be the back–propagation of the decomposed wave field using the Gaussian packet method and the construction of the migrated section.

Acknowledgements

The author is greatly indebted to Luděk Klimeš for guidance throughout the work on this topic.

References

Babich, V. M. & Ulin, V. V. (1981): Complex space time ray method and 'quasiphotons'. Zap. Nauchn. Sem. Leningr. Otd. Math. Inst., **117**, 5–12 (in Russian); English transl.: J.Sov. Math., **24**, 269–273, 1984.

Klimeš, L. (1989a): Gaussian packets in the computation of seismic wavefields. Geophys. J. Int., **99**, 421–433.

Klimeš, L. (1989b): Optimization of the shape of Gaussian beams of a fixed length. Stud. geophys. geod., **33**, 146–163.

Ralston, J. (1983): Gaussian beams and the propagation of singularities. MAA Studies in Mathematicc., **23**, 206–248.

Versteeg, R. J. & Grau, G. (eds.) (1991): The Marmousi experience. Proc. EAGE workshop on Practical Aspects of Seismic Data Inversion (Copenhagen, 1990), Eur. Assoc. Explor. Geophysicists, Zeist.

Žáček, K. (2001): Optimization of the shape of Gaussian beams. In: Seismic Waves in Complex 3–D Structures, Report 11, Charles University, Prague, 181–201.

Žáček, K. (2002): Smoothing the Marmousi model. Pure and appl. Geophys., **159**, 1507–1526.